

## Three-Bond Sugar–Base Couplings in Purine *versus* Pyrimidine Nucleosides: A DFT Study of Karplus Relationships for ${}^3J_{C2/4-H1'}$ and ${}^3J_{C6/8-H1'}$ in DNA

Markéta L. Munzarová\* and Vladimír Sklenář\*

National Centre for Biomolecular Research, Faculty of Science, Masaryk University, Kotlářská 2, CZ-611 37 Brno, Czech Republic

Received April 11, 2002

The glycosidic torsion angle  $\chi$  defines the orientation of the aromatic base with respect to the ribose (RNA) or 2'-deoxyribose (DNA) moiety in purine and pyrimidine nucleotides. Its knowledge is a prerequisite in structure determination of nucleic acids. A number of methods have been developed to determine the  $\chi$  values using NMR data, of which only the quantitative evaluation of the interproton NOEs<sup>1</sup> and the measurement of three-bond carbon-proton scalar couplings across the glycosidic bond<sup>2–5</sup> have been widely used.  ${}^3J_{C2/4-H1'}$  and  ${}^3J_{C6/8-H1'}$  constants can be employed for quantitative determination of  $\chi$ , providing the correct Karplus-type relationship between the scalar couplings and  $\chi$  is known.<sup>5–8</sup> A quantum-chemical study reported here shows that, in contrast to the known *trans* to *cis* ratio of couplings ( ${}^3J_{C6/8-H1'(cis)} < {}^3J_{C6/8-H1'(trans)}$ ) for purine nucleosides, the opposite ratio is to be expected for pyrimidine nucleosides ( ${}^3J_{C6/8-H1'(cis)} > {}^3J_{C6/8-H1'(trans)}$ ).<sup>9</sup> An analysis of the FPT-DFT results in terms of canonical MO contributions suggests that the unusual three-bond coupling may be attributed to a through-space contribution to  ${}^3J_{C6/8-H1'}$  in the *syn* orientation that is very effective for pyrimidine nucleosides and considerably weaker for purine nucleosides.

Previous experimental studies of the Karplus relationships for  ${}^3J_{C2/4-H1'}$  and  ${}^3J_{C6/8-H1'}$ <sup>5–7</sup> utilized the data covering only relatively narrow regions of  $\chi$ . In addition, no experimental data are available for *syn* oriented pyrimidines. To overcome these limitations, we have decided to compare the Karplus curves for purine and pyrimidine nucleosides using a theoretical approach. While the results reporting unusual through-space mechanism of spin–spin scalar interactions are presented in this communication, additional data and their analysis will be published elsewhere.<sup>10</sup> We have performed a series of  ${}^3J_{C2/4-H1'}$  and  ${}^3J_{C6/8-H1'}$  calculations for deoxyadenosine (A), deoxyguanosine (G), deoxycytidine (C), and deoxythymidine (T) with  $\chi$  varying from  $-180^\circ$  to  $+180^\circ$ . These couplings were calculated by a combined SOS-DFPT (for the PSO and DSO terms) and DFT/FPT (for the FC term) approach as implemented in the deMon-NMR code.<sup>11</sup>

Our DFT results show that the C2/4–H1' interaction is, except for T, not very sensitive to the base type. For the *anti* glycosidic torsion ( $\chi \approx -120^\circ$ ), its maximal magnitude is between 2 and 2.1 Hz for A, C, G, and 2.7 Hz for T. For the *syn* torsion ( $\chi \approx 60^\circ$ ), the maximum of  ${}^3J_{C2/4-H1'}$  is between 5.5 and 5.7 Hz for A, C, G and 6.9 Hz for T. A significant difference between purine and pyrimidine bases, however, is found for  ${}^3J_{C6/8-H1'}$ . While the maximal C6/8–H1' interaction in the *anti* region is only by ca. 0.5 Hz weaker for pyrimidine than for purine (4.3–4.5 Hz for A, G *versus* 3.9–4.0 Hz for C, T), in the *syn* region the scalar coupling

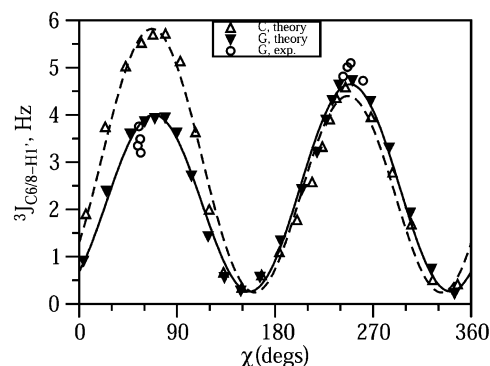


**Figure 1.**  ${}^3J_{C6/8-H1'}$  coupling as a function of  $\chi$  for deoxycytidine (C) and deoxyguanosine (G). Theoretical results refer to the present work, and experimental results refer to ref 5.

for pyrimidine is substantially, by about 2 Hz, stronger (5.7 Hz for C, T *versus* 3.9 Hz for A, G). For G, this result compares well with the experiment (cf. Figure 1). The calculated data predict a novel trend in the case of C, T, for which no NMR results are available in the *syn* region. Although the experimental  ${}^3J_{C6/8-H1'}$  for modified pyrimidine bicyclo nucleosides is close to that for genuine purine nucleosides,<sup>5–7</sup> the bond formation at O2 may influence  ${}^3J_{C6/8-H1'}$  to an extent that makes the comparison with genuine pyrimidine nucleosides irrelevant (cf. below).

The most striking feature of Figure 1 is the qualitatively different dependence of  ${}^3J_{C6/8-H1'}$  on  $\chi$  when comparing pyrimidine and purine nucleosides. While  ${}^3J_{C6/8-H1'(cis)} < {}^3J_{C6/8-H1'(trans)}$  for G, the reversed, much less usual relation<sup>12</sup> holds for C. To understand the behavior of  ${}^3J_{C6/8-H1'}$  in pyrimidine nucleosides, we have decomposed the FC term into contributions of pairs of the spin-polarized molecular orbitals (MOs) and studied them as a function of the base type.<sup>13</sup> Our interest was focused mainly on the *syn* glycosidic torsion ( $\chi = 60^\circ$ ), to which all of the results presented in this paragraph refer. First, we note that the core orbitals make negligible ( $<0.1$  Hz) contributions to the studied coupling. Approximately in the middle of the energy spectrum of the occupied MOs, there is a broad band of orbitals that give large (up to tenths of Hz), mutually compensating contributions to  ${}^3J_{C6/8-H1'}$ . The corresponding MOs possess a  $\sigma_{H1'-C1'}$  and  $\sigma_{N1-C6/8}$  character. The compensation of the contributions is not complete, though, and, for the purine nucleosides, the difference accounts for the key fraction of the observed coupling. For the pyrimidine nucleosides, however, there are important additional contributions stemming from the occupied frontier molecular orbitals (FMOs). For C, the contributions of the HOMO (10.3 Hz) and the HOMO-1 ( $-6.9$  Hz) add up to a coupling of 3.4 Hz.<sup>14</sup> Figure 2 shows the character of the two FMOs in their simplified, EHT representation<sup>15</sup> that highlights the covalent

\* To whom correspondence should be addressed. E-mail: (M.L.M.) marketa@ncbr.chemi.muni.cz; (V.S.) sklenar@chemi.muni.cz.

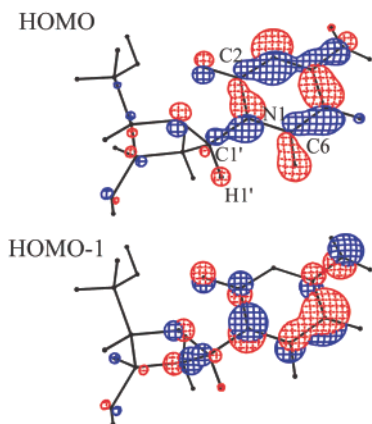


**Figure 2.** Two highest occupied molecular orbitals of deoxycytidine.

character of the bonds involved in the coupling pathway. The DFT-counterparts of the displayed MOs have qualitatively the same bonding characteristics; the main quantitative difference is a major (60%) localization of the HOMO at O2 of the base with important consequences discussed below. For T, the pair of the significantly contributing MOs is shifted two levels down in energy, but the four highest-occupied MOs give the same net contribution (3.4 Hz) as discussed above for C. On the contrary, the corresponding net contributions in purines are only 0.8 Hz for G and 0.4 Hz for A.

Note that HOMO and HOMO-1 of C clearly have a  $\pi_{N1-C6}^*$  character. The relatively small participation of C1' in these MOs (0.5%, DFT results) opens the question if the H1'–C6 spin–spin coupling path mediated by the FMOs passes through C1' or not. The net Mulliken spin populations indicate that within the HOMO, a net “up” spin at H1' generates comparable amounts of net “down” spin at N1 and net “up” spin at C6, and somewhat less net “up” spin at C1'. The spin populations arising from HOMO-1 are of exactly opposite signs but smaller magnitudes. Therefore, the distribution of “up” and “down” spin within the HOMO, HOMO-1 pair is qualitatively the same as for HOMO itself. The sign of the net spin is switched between H1' and N1 and between N1 and C6, but not between H1' and C1'. Thus, the spin transfer from H1' to C6 does not follow a sequence of three one-bond coupling steps H1'–C1', C1'–N1, N1–C6, where the sign of the spin would be switched between each of the two coupled atoms. The latter requirement is, however, fulfilled for the H1'–N1', N1'–C6 coupling pathway. From this and from the strong dependence of FMO contributions on  $\chi$  (cf. below), we conclude that the HOMO, HOMO-1 pair corresponds to H1'–N1–C6 contribution to  ${}^3J_{C6/8-H1'}$  coupling that may have partially through-space character. This mechanism can be related to the recently introduced NBO-based interpretation of spin–spin coupling<sup>16</sup> in terms of a  $\sigma_{H1'-C1'} \rightarrow \pi_{N1-C6}^*$  hyperconjugation.<sup>17</sup>

As a function of  $\chi$ , the HOMO contribution to  ${}^3J_{C6/8-H1'}$  is maximized for the *syn* orientation displayed at Figure 2 and is significantly smaller (1.5 Hz) for the *anti* orientation. However, the magnitude of the hyperconjugative contribution to  ${}^3J_{C6/8-H1'}$  depends also on the participation of C6/C8 orbitals in the HOMO, which is for pyrimidines larger than for purines. For purines, the electron density in the HOMO is withdrawn from C8 to its two more electronegative neighbors, N9 and N7. This explains the small through-space contribution and the *trans* to *cis* ratio of  ${}^3J_{C6/8-H1'}$  for A and G.

Finally, let us estimate the consequence of the deoxycytidine HOMO shape for the spin–spin coupling in the modified bicyclo nucleosides (cf. above). This orbital possesses 60% of O2 lone-pair character and is therefore expected to be involved in a major orbital interaction upon the bond formation between O2 and a sugar atom. It may be anticipated that such a bond formation has an influence on  ${}^3J_{C6/8-H1'}$  to which HOMO largely contributes. Indeed, our theoretical results (cf. Supporting Information) for experimentally studied uridine bicyclo compounds<sup>6</sup> demonstrate that the smaller  ${}^3J_{C6/8-H1'}$  in the bicyclo as compared to genuine pyrimidine nucleosides is due to the missing through-space contributions. More detailed study and parameters of the Karplus equations for individual nucleosides will be published elsewhere.

**Acknowledgment.** This work was supported by grant LN00A016 from the Ministry of Education of the Czech Republic. We are grateful to Dr. Olga L. Malkina for the software package for FC-MO analysis and helpful discussions.

**Supporting Information Available:** Computational details, computed structures, table of FC, PSO, and DSO contributions, comparison of results for S and N sugar conformation, computed  ${}^3J_{C2-H1'}$  and  ${}^3J_{C6-H1'}$  for uridine bicyclo compounds (PDF), plots of  ${}^1J_{C1'-H1'}$  versus  $\chi$  for C, G (PS). This material is available free of charge via the Internet at <http://pubs.acs.org>.

## References

- (1) Wijmenga, S. S.; van Buuren, B. N. M. *Prog. Nucl. Magn. Reson. Spectrosc.* **1998**, *32*, 287.
- (2) Zhu, G.; Live, D.; Bax, A. *J. Am. Chem. Soc.* **1994**, *116*, 8370–8371.
- (3) Schwalbe, H.; Marino, J. P.; King, G. C.; Wechselberger, R.; Bernel, W.; Griesinger, C. *J. Biomol. NMR* **1994**, *4*, 631–644.
- (4) Zimmer, D. P.; Marino, J. P.; Griesinger, C. *Magn. Reson. Chem.* **1996**, *34*, S177–S186.
- (5) Trantírek, L.; Štefl, R.; Masse, J. E.; Feigon, J.; Sklenář, V. *J. Biomol. NMR* **2002**, *23*, 1.
- (6) Davies, D. B.; Rajani, P.; MacCoss, M.; Danylyuk, S. *Magn. Reson. Chem.* **1985**, *23*, 72–77.
- (7) Ippel, J. H.; Wijmenga, S. S.; de Jong, R.; Heus, H. A.; Hilbers, C. W.; de Vroom, E.; van der Marel, G. A.; van Boom, J. H. *Magn. Reson. Chem.* **1996**, *34*, S156–S176.
- (8) Karplus, M. *J. Am. Chem. Soc.* **1963**, *85*, 2870.
- (9) In this work, “*cis*” and “*trans*” (used in connection with  ${}^3J_{C6/8-H1'}$ ) refer to the dihedral angle C6/8–N1/9–C1'–H1'.
- (10) Munzarová, M. L.; Sklenář, V., manuscript in preparation.
- (11) (a) Salahub, D. R.; Fournier, R.; Mlynarski, P.; Papai, I.; St-Amant, A.; Ushio, J. In *Density Functional Methods in Chemistry*; Labanowski, J., Andzelm, J., Eds.; Springer: New York, 1991. (b) Malkin, V. G.; Malkina, O. L.; Eriksson, L. A.; Salahub, D. R. In *Modern Density Functional Theory: A Tool for Chemistry*; Seminario, J. M., Politzer, P., Eds.; Elsevier: Amsterdam, 1995; Vol. 2. (c) Malkin, V. G.; Malkina, O.; Casida, M. E.; Salahub, D. R. *J. Am. Chem. Soc.* **1994**, *116*, 5898.
- (12) Contreras, R. H.; Peralta, J. E. *Prog. Nucl. Magn. Reson. Spectrosc.* **2000**, *37*, 321.
- (13) The PSO and DSO terms represent for all systems less than 4% of the total  ${}^3J_{C6/8-H1'}$ .
- (14) The next 11 MOs give small (<1 Hz), mutually compensating contributions to  ${}^3J_{C6/8-H1'}$  and separate the FMOs from the other contributing MOs.
- (15) Mealli, C.; Proserpio, D. M. *J. Chem. Educ.* **1990**, *67*, 399. EHT energies of HOMO and HOMO-1 are switched as compared to DFT results.
- (16) (a) Peralta, J. E.; Contreras, R. H.; Snyder, J. P. *Chem. Commun.* **2000**, 20, 2025. Peralta, J. E.; Barone, V.; Contreras, R. H. *J. Am. Chem. Soc.* **2001**, *123*, 9162. (b) Wilkens, S. J.; Westler, W. M.; Markley, J. L.; Weinhold, F. *J. Am. Chem. Soc.* **2001**, *123*, 12026.
- (17) While HOMO and HOMO-1 include a small fraction of electrons in  $\sigma_{H1'-C1'}$ , they're the only occupied MOs having significant  $\pi_{N1-C6}^*$  character. They thus represent most of the  $\sigma_{H1'-C1'} \rightarrow \pi_{N1-C6}^*$  interaction. Interestingly, the related weakening of the  $\sigma_{H1'-C1'}$  bond for the *syn* as compared to the *anti* torsion is reflected in a considerable decrease of  ${}^1J_{H1'-C1'}$ , cf., Supporting Information.

JA026502P